κ-Deformed Schwarzschild–AdS Black Strings as Holographic Heat Engines

Dhruba Jyoti Gogoi[1], **Sandeep Lama**[2,*], **Poppy Hazarika**[2], **Jyatsnasree Bora**[1]

[1]Department of Physics, Madhabdev University, Narayanpur, Lakhimpur 784164, Assam, India | [2]Department of Physics, Duliajan College, Duliajan 786602, Assam, India

*Corresponding Email: moloydhruba@yahoo.in | sandeeplama2004@gmail.com | poppyhazarika1@gmail.com | jyatnasree.borah@gmail.com

1. Motivation & κ-Deformed Spacetime

- **Black Hole Chemistry & Holography:** Promoting the negative cosmological constant to thermodynamic pressure $P = -\Lambda/(8\pi)$ reinterprets the black string ADM mass per unit length as gravitational enthalpy ($H = M = U + PV$). Cyclic processes in the (P, V) plane operate as **holographic heat engines**, charting renormalization-group (RG) trajectories across a continuous family of dual large-N boundary CFTs.
- **κ-Minkowski Noncommutativity:** Planck-scale quantum-gravitational structure is encoded via Lie-algebraic spacetime commutation relations governed by κ-Poincaré symmetry:

$$[\hat{x}^i, \hat{x}^0] = ia\hat{x}^i, \qquad [\hat{x}^i, \hat{x}^j] = 0,$$

where $a \geq 0$ is the fundamental minimal length deformation scale.

- **κ-Modified Potential & Anisotropic Source:** Replacing the classical point singularity via $V_{\rm N}(r) = -\frac{M}{r}\left(1 - \frac{aM}{12\pi r^2}\right)$ sources an effective anisotropic fluid stress-energy tensor ($\nabla_\mu T^\mu_{\ \nu} = 0$):

$$T^0_{\ 0} = T^1_{\ 1} = -\frac{aM^2}{8\pi^2 r^5}, \qquad T^2_{\ 2} = T^3_{\ 3} = \frac{3aM^2}{16\pi^2 r^5}$$

which satisfies the null, weak, and strong energy conditions for $a > 0$.

2. Cylindrical Black String & Horizons

Following Lemos's cylindrically symmetric ansatz ($\mathbb{R} \times S^1$ horizon topology):

$$ds^2 = -f(r)\,dt^2 + \frac{dr^2}{f(r)} + r^2\left(d\phi^2 + \alpha^2 dz^2\right).$$

Integrating the radial Einstein–Λ equations $G_\mu^{\ \nu} + \Lambda\delta_\mu^{\ \nu} = 8\pi T_\mu^{\ \nu}$ yields the exact κ-deformed metric lapse function:

$$f(r) = -\frac{2M}{r} + \underbrace{\frac{aM^2}{2\pi r^3}}_{\text{Repulsive NC Core}} + \frac{8\pi P}{3}r^2, \qquad P = -\frac{\Lambda}{8\pi}$$

- **Curvature Invariants ($r = 0$ Singularity Strengthened to r^{-10}):**

$$R = 4\Lambda - \frac{aM^2}{\pi r^5}, \qquad \lim_{r\to\infty} R = 4\Lambda,$$
$$K(r) = \frac{8\Lambda^2}{3} - \frac{4\Lambda a M^2}{3\pi r^5} + \frac{48M^2}{r^6} - \frac{80aM^3}{\pi r^8} + \frac{46a^2M^4}{\pi^2 r^{10}}.$$

- **Horizon Splitting & Cosmic Censorship Bound:** Analyzing $\mathcal{P}(r) = r^5 + \frac{6M}{\Lambda}r^2 - \frac{3aM^2}{2\pi\Lambda}$ with minimum at $r_{\rm min} = (-12M/5\Lambda)^{1/3}$ shows that the repulsive $\mathcal{O}(ar^{-3})$ core splits the single Lemos horizon into an inner Cauchy horizon r_- and an outer event horizon r_+ for $0 < a \leq a_{\rm max}$:

$$a \leq a_{\rm max} \equiv \frac{12\pi}{5M^{1/3}}\left(-\frac{12}{5\Lambda}\right)^{2/3} = \frac{12\pi}{5M^{1/3}}\left(\frac{3}{10\pi P}\right)^{2/3}$$

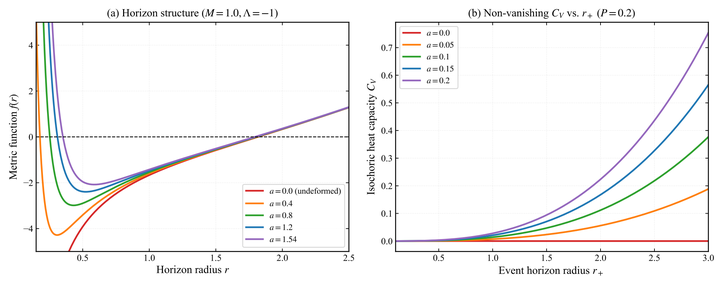

Fig. 1: (a) Radial profile of $f(r)$ ($M = 1.0, \Lambda = -1$) showing horizon splitting, and (b) isochoric heat capacity $C_V(r_+)$ for $P = 0.2$ showing $C_V > 0$ for $a > 0$.

3. Extended Phase-Space Chemistry

Evaluated per unit effective longitudinal string length (αl_z) to $\mathcal{O}(a)$:

Wald Entropy: $S = \frac{\pi r_+^2}{2}\left(1 + \frac{4aPr_+}{9}\right) = \frac{\pi}{2}\left(\frac{3V}{2\pi}\right)^{2/3} + \frac{aPV}{3}$

ADM Enthalpy: $M = \frac{2\pi P r_+^3}{3}\left(1 + \frac{aPr_+}{3}\right), \qquad V = \left(\frac{\partial M}{\partial P}\right)_{S,a} = \frac{2\pi r_+^3}{3}$

Hawking Temp.: $T = 2Pr_+\left(1 - \frac{2aPr_+}{9}\right), \qquad \Phi_a = \left(\frac{\partial M}{\partial a}\right)_{S,P} = -\frac{2\pi P r_+^4}{9}$

- **Extended First Law, Smarr Formula & Equation of State:**

$$dM = T\,dS + V\,dP + \Phi_a\,da, \qquad M = 2ST - 2PV + a\Phi_a,$$
$$P(r_+, T) = \frac{9 - \sqrt{81 - 36aT}}{4ar_+} = \frac{T}{2r_+}\left(1 + \frac{aT}{9} + \mathcal{O}(a^2)\right).$$

- **Global Stability:** With $C_P = \pi r_+^2\left(1 + \frac{8aPr_+}{9}\right) > 0$, $G = -\frac{\pi P r_+^3}{3} < 0$, and $(\partial P/\partial V)_T < 0$, there are **no Hawking–Page or van der Waals P–V transitions**.

Strict Physical Monotonicity Domain: $0 < aPr_+ < \frac{9}{4} = 2.25$

4. Non-Vanishing Isochoric Specific Heat ($C_V > 0$)

In conventional static black hole heat engines, $S = S(r_+)$ and $V = V(r_+)$ depend solely on r_+, implying $C_V = 0$ and making isochores strictly adiabatic ($\delta Q_{\rm isochore} = 0$).

For the κ-deformed black string, the Wald entropy $S(V, P, a)$ depends **explicitly on pressure** P at fixed horizon radius r_+:

$$\left(\frac{\partial S}{\partial P}\right)_{V,a} = \frac{2\pi a r_+^3}{9} = \frac{aV}{3} > 0, \qquad C_V = T\frac{(\partial S/\partial P)_{V,a}}{(\partial T/\partial P)_{V,a}}.$$

Expanding consistently to first order in a yields a strictly positive specific heat:

$$\boxed{C_V = \frac{2\pi a P r_+^3}{9} + \mathcal{O}(a^2) = \frac{aPV}{3} + \mathcal{O}(a^2) > 0}$$

- **Non-Adiabatic Isochores:** Vertical branches in the P–V plane actively exchange heat with the thermal reservoirs ($C_V \propto r_+^3$, see Fig. 1(b)).
- **Breaking of Carnot–Stirling Degeneracy:** Because isochoric pressurization absorbs heat $Q_{\rm isochore,in} = \frac{\pi a r_1^2}{18}(T_H^2 - T_C^2) > 0$, the classical equivalence between Stirling and Carnot cycles is broken at $\mathcal{O}(a)$:

$$\eta_{\rm Stirling} = \frac{W_{\rm Stirling}}{Q_{{\rm iso},H} + Q_{\rm isochore,in}} < 1 - \frac{T_C}{T_H} = \eta_C.$$

5. Rectangular P–V Cycle & Heat Flows

We drive the black string around a rectangular cycle $1 \to 2 \to 3 \to 4 \to 1$ between pressures (P_4, P_1) and horizon radii (r_1, r_2) at fixed a:

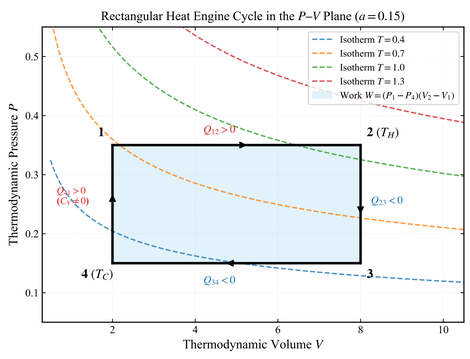

Fig. 2: Rectangular holographic heat engine cycle $1 \to 2 \to 3 \to 4 \to 1$ overlaid on the P–V isotherms ($a = 0.15$) with net work $W = \frac{2\pi}{3}(P_1 - P_4)(r_2^3 - r_1^3)$.

Branch	Fixed	Exact Heat Flow $\delta Q = T\,dS$	Sign
$1 \to 2$	P_1	$Q_{12} = \frac{2\pi P_1}{3}(r_2^3 - r_1^3) + \frac{2\pi a P_1^2}{9}(r_2^4 - r_1^4)$	+ (In)
$2 \to 3$	r_2	$Q_{23} = \frac{2\pi a r_2^4}{9}(P_4^2 - P_1^2)$	− (Out)
$3 \to 4$	P_4	$Q_{34} = \frac{2\pi P_4}{3}(r_1^3 - r_2^3) + \frac{2\pi a P_4^2}{9}(r_1^4 - r_2^4)$	− (Out)
$4 \to 1$	r_1	$Q_{41} = \frac{2\pi a r_1^4}{9}(P_1^2 - P_4^2)$	+ (In)

6. Exact Thermal Efficiency & Carnot Ratio

Summing the heat inputs ($Q_H = Q_{12} + Q_{41}$) and heat rejections ($Q_C = -Q_{23} - Q_{34}$), the intermediate enthalpies M_1 and M_3 cancel identically ($Q_H - Q_C = W$):

$$Q_C = (M_2 - M_4) - V_2(P_1 - P_4) = \frac{2\pi P_4}{3}\left(r_2^3 - r_1^3\right) + \frac{2\pi a}{9}\left(P_1^2 r_2^4 - P_4^2 r_1^4\right).$$

Dividing net work $W = \frac{2\pi}{3}(P_1 - P_4)(r_2^3 - r_1^3)$ by Q_H yields the exact efficiency:

$$\eta = \frac{W}{Q_H} = \frac{(P_1 - P_4)(r_2^3 - r_1^3)}{P_1(r_2^3 - r_1^3) + \frac{a}{3}(P_1^2 r_2^4 - P_4^2 r_1^4)}$$
$$= \eta_0\left[1 - \frac{a(P_1^2 r_2^4 - P_4^2 r_1^4)}{3P_1(r_2^3 - r_1^3)}\right] + \mathcal{O}(a^2), \qquad \eta_0 \equiv 1 - \frac{P_4}{P_1}$$

Benchmarking against the Carnot efficiency $\eta_C = 1 - T_C/T_H$ between $T_H = T(r_2, P_1)$ and $T_C = T(r_1, P_4)$:

$$\eta_C = 1 - \frac{P_4 r_1\left(1 - \frac{2aP_4 r_1}{9}\right)}{P_1 r_2\left(1 - \frac{2aP_1 r_2}{9}\right)} = \eta_{C,0} - \frac{2aP_4 r_1}{9P_1 r_2}(P_1 r_2 - P_4 r_1) + \mathcal{O}(a^2)$$

$$\frac{\eta}{\eta_C} = \left(\frac{1 - P_4/P_1}{1 - \frac{P_4 r_1}{P_1 r_2}}\right)\left[1 - \frac{a}{9}\left(\frac{3(P_1^2 r_2^4 - P_4^2 r_1^4)}{P_1(r_2^3 - r_1^3)} - 2P_4 r_1\right)\right] + \mathcal{O}(a^2)$$

7. Quantitative Benchmarks ($r_1 = 1.0, P_1 = 0.4, P_4 = 0.1$)

a	r_2	$C_V(r_2, P_1)$	Q_{41}	η	η_C	η/η_C
0.00	2.0	0.0000	0.0000	0.7500	0.8750	0.8571
0.05	2.0	0.1117	0.0052	0.7390	0.8740	0.8455
0.10	2.0	0.2234	0.0105	0.7283	0.8730	0.8343
0.15	2.0	0.3351	0.0157	0.7179	0.8719	0.8234
0.20	2.0	0.4468	0.0209	0.7078	0.8708	0.8128
0.20	3.0	1.5080	0.0209	0.6808	0.9125	0.7461

8. Performance Analysis & Scaling Trends

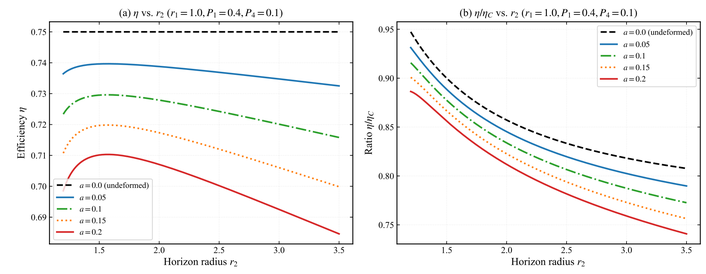

Fig. 3: Variation of (a) η and (b) η/η_C vs. outer horizon radius r_2 ($r_1 = 1.0, P_1 = 0.4, P_4 = 0.1$).

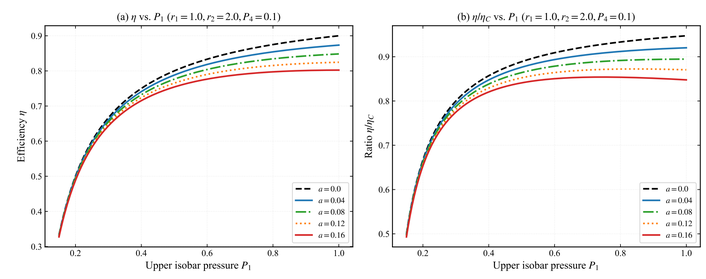

Fig. 4: Variation of (a) η and (b) η/η_C vs. upper operating pressure P_1 ($r_1 = 1.0, r_2 = 2.0, P_4 = 0.1$).

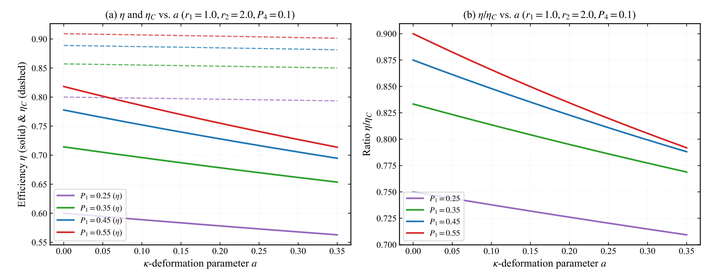

Fig. 5: Direct dependence of (a) η and η_C and (b) η/η_C on deformation parameter a.

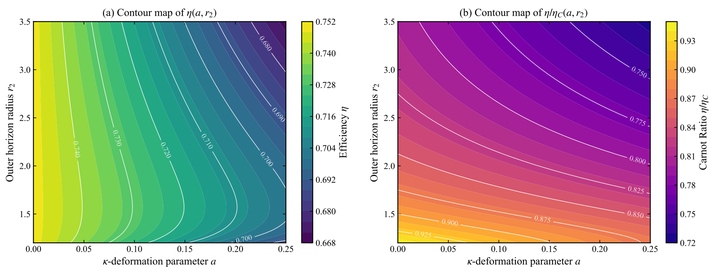

Fig. 6: 2D phase-space contour maps of (a) $\eta(a, r_2)$ and (b) $\eta/\eta_C(a, r_2)$.

9. Results and Discussions

- **Active Isochoric Heat Transfer ($C_V > 0$):** Unlike commutative Lemos black strings ($a = 0, C_V = 0$) where isochores are adiabatic, the pressure-dependent Wald entropy $S(V, P, a)$ yields $C_V = aPV/3 > 0$. Consequently, the left isochore absorbs heat $Q_{41} = \frac{2\pi a r_1^4}{9}(P_1^2 - P_4^2) > 0$ and the right isochore rejects a larger heat $|Q_{23}| = \frac{2\pi a r_2^4}{9}(P_1^2 - P_4^2) > Q_{41}$, breaking Carnot–Stirling degeneracy ($\eta_{\rm Stirling} < \eta_C$).
- **Breakdown of Horizon-Scale Invariance:** At $a = 0$, $\eta_0 = 1 - P_4/P_1$ is independent of (r_1, r_2). For $a > 0$, the quartic heat penalty $\Delta Q_H \propto a(P_1^2 r_2^4 - P_4^2 r_1^4)$ outpaces cubic mechanical work $W \propto (r_2^3 - r_1^3)$, causing η and η/η_C to decrease monotonically with r_2, approaching $\eta \simeq \eta_0(1 - aP_1 r_2/3)$ for $r_2 \gg r_1$.
- **Pressure Boosting vs. NC Suppression:** Increasing the source pressure P_1 enhances η and η/η_C across all a, whereas increasing a linearly suppresses both metrics while strictly preserving the Second Law ($0 < \eta < \eta_C < 1$).
- **Holographic RG Flow Interpretation:** Varying P corresponds to changing the central charge $c \propto P^{-1}$ of the dual cylindrical CFT. Bulk κ-noncommutativity excites internal UV degrees of freedom during isochoric RG flows ($4 \to 1$) that absorb heat $Q_{41} > 0$ without contributing to mechanical work.

10. Conclusions & Holographic Implications

1. **Pressure-Dependent Entropy & $C_V > 0$:** Because $S = \frac{\pi r_+^2}{2}\left(1 + \frac{4aPr_+}{9}\right)$ depends on P at fixed volume $V = \frac{2\pi r_+^3}{3}$, the isochoric specific heat $C_V = \frac{2\pi a P r_+^3}{9} > 0$ is strictly positive, making isochores non-adiabatic and breaking Carnot–Stirling degeneracy ($\eta_{\rm Stirling} < \eta_C$).
2. **Quantum Suppression:** Noncommutativity introduces a quartic heat penalty $\Delta Q_H \propto a(P_1^2 r_2^4 - P_4^2 r_1^4)$ that monotonically suppresses η and η/η_C as a or r_2 increases, while strictly obeying $\eta < \eta_C < 1$.
3. **AdS/CFT Interpretation:** Bulk κ-deformation manifests in the dual cylindrical CFT as extra internal degrees of freedom that absorb heat during RG-flow pressurization ($4 \to 1$) without performing mechanical work.

References:

[1] C. V. Johnson, *Class. Quant. Grav.* **31**, 205002 (2014);

[2] J. P. S. Lemos, *Phys. Lett. B* **353**, 46 (1995);

[3] B. Eslam Panah *et al.*, κ-Deformed Schwarzschild–AdS Black Strings (2026).

Ack.: COST Action CA21136 (CosmoVerse).